Loss of *Protocadherin-12* Leads to Diencephalic-Mesencephalic Junction Dysplasia Syndrome

Alicia Guemez-Gamboa, PhD,[1] Ahmet Okay Çağlayan, MD,[2] Valentina Stanley, BS,[3] Anne Gregor, PhD,[1] Maha S. Zaki, MD, PhD,[4] Sahar N. Saleem, MBBCH, MSc, MD,[5] Damir Musaev, BS,[3] Jennifer McEvoy-Venneri, BS,[3] Denice Belandres, BS,[3] Naiara Akizu, PhD,[3] Jennifer L. Silhavy, MS,[3] Jana Schroth, BS,[3] Rasim Ozgur Rosti, MD,[1] Brett Copeland, BS,[1] Steven M. Lewis, BS,[1] Rebecca Fang, BS,[1] Mahmoud Y. Issa, MD, PhD,[4] Huseyin Per, MD,[6] Hakan Gumus, MD,[6] Ayse Kacar Bayram, MD,[6] Sefer Kumandas, MD,[6] Gozde Tugce Akgumus, MS,[7] Emine Z. Erson-Omay, PhD,[7] Katsuhito Yasuno, PhD,[7] Kaya Bilguvar, MD,[7] Gali Heimer, MD, PhD,[8] Nir Pillar, MD,[8] Noam Shomron, PhD,[8] Daphna Weissglas-Volkov, PhD,[8] Yuval Porat, PhD,[9] Yaron Einhorn, MSc,[9] Stacey Gabriel, PhD,[10] Bruria Ben-Zeev, MD,[8] Murat Gunel, MD,[2] and Joseph G. Gleeson, MD [1,3]

Objective: To identify causes of the autosomal-recessive malformation, diencephalic-mesencephalic junction dysplasia (DMJD) syndrome.

Methods: Eight families with DMJD were studied by whole-exome or targeted sequencing, with detailed clinical and radiological characterization. Patient-derived induced pluripotent stem cells were derived into neural precursor and endothelial cells to study gene expression.

Results: All patients showed biallelic mutations in the nonclustered *protocadherin-12* (*PCDH12*) gene. The characteristic clinical presentation included progressive microcephaly, craniofacial dysmorphism, psychomotor disability, epilepsy, and axial hypotonia with variable appendicular spasticity. Brain imaging showed brainstem malformations and with frequent thinned corpus callosum with punctate brain calcifications, reflecting expression of *PCDH12* in neural and endothelial cells. These cells showed lack of *PCDH12* expression and impaired neurite outgrowth.

Interpretation: DMJD patients have biallelic mutations in *PCDH12* and lack of protein expression. These patients present with characteristic microcephaly and abnormalities of white matter tracts. Such pathogenic variants predict a poor outcome as a result of brainstem malformation and evidence of white matter tract defects, and should be added to the phenotypic spectrum associated with *PCDH12*-related conditions.

ANN NEUROL 2018;84:646–655

View this article online at wileyonlinelibrary.com. DOI: 10.1002/ana.25327

Received Nov 8, 2017, and in revised form Aug 27, 2018. Accepted for publication Aug 29, 2018.

Address correspondence to Dr Joseph G. Gleeson, Howard Hughes Medical Institute, Laboratory for Pediatric Brain Disease, Rockefeller University, 1230 York Avenue, New York, NY 10065. E-mail: jogleeson@rockefeller.edu

From the [1]Howard Hughes Medical Institute, Laboratory for Pediatric Brain Disease, Rockefeller University, New York, NY; [2]Department of Neurosurgery, Yale School of Medicine, New Haven, CT; [3]Department of Neurosciences, University of California, San Diego, La Jolla, CA; [4]Department of Clinical Genetics, National Research Centre, Cairo, Egypt; [5]Radiology Department-Faculty of Medicine, Cairo University, Cairo, Egypt; [6]Department of Paediatrics, Division of Paediatric Neurology, School of Medicine, Erciyes University, Kayseri, Turkey; [7]Departments of Neurosurgery, Neurobiology and Genetics, Yale School of Medicine, New Haven, CT; [8]Sackler School of Medicine, Tel Aviv University, Tel Aviv, Israel; [9]Genoox, Tel Aviv, Israel; and [10]Broad Institute of Harvard and Massachusetts Institute of Technology, Cambridge, MA

Additional supporting information may be found online in the Supporting Information section at the end of the article.

We reported on a new clinical condition, diencephalic-mesencephalic junction dysplasia (DMJD), characterized by a distinctive brainstem "butterfly sign" on axial computed tomography (CT)/magnetic resonance (MR) images. Although the genetic basis was not previously known, clinical data suggested a unique developmental brainstem defect.[1] The butterfly sign was attributed to an anterior midbrain cleft contiguous with the third ventricle, along with downward displacement of the diencephalic-mesencephalic junction. In DMJD patients studied with tractography, the corticospinal tract (CST), which originates in the cortical motor area and normally courses medially to project to the contralateral spinal cord, instead coursed laterally and appeared to terminate prematurely. A defect in CST function was clinically evidenced by spasticity of the limbs accompanied by quadriparesis. Additionally, thinned corpus callosum in the majority of subjects supported a white matter tract developmental defect. Since the original publication, several reports of additional patients with DMJD have appeared,[2–4] suggesting a unique radiographically defined condition, but the genetic basis remained unknown.

Here, we analyzed two of the originally described DMJD families and found biallelic loss-of-function variants in *protocadherin-12* (*PCDH12*). Moreover, we identify six additional families for a total of eight independent families representing 14 patients carrying pathogenic variants in *PCDH12. PCDH12* belongs to the nonclustered group of the protocadherin family, the largest group within the cadherin superfamily,[5,6] encoding an 1,184-amino-acid (aa) glycoprotein with six cadherin domains, a transmembrane domain, and an intracellular domain. PCDH12 was originally identified in endothelioma cell lines,[7] where it concentrates at cell-cell junctions and promotes cell adhesion.[8,9]

Protocadherins are diversified cell-surface proteins with over 70 members that are part of the cadherin superfamily. The protocadherin family is subdivided into the clustered and nonclustered groups based on their genomic organization.[5,6] Correlated expression patterns of nonclustered protocadherins suggest roles in neural circuit formation,[10,11] and several nonclustered protocadherin genes have been implicated in neurological diseases. Pathogenic variants in the X-linked *PCDH19* cause female-specific epilepsy with mental retardation (MIM#300088).[12,13] *PCDH8, -9*, and *-10* have been linked to autism,[14–16] *PCDH7* has been linked to epilepsy,[17] and *PCDH17* variants confer a risk for mood disorders.[18] *PCDH12* variants have been associated with schizophrenia,[19] and recently biallelic pathogenic variants have been linked to microcephaly, seizures, spasticity with brain calcifications [OMIM#251280].[20,21] Our report extends the phenotypic spectrum associated with *PCHD12* mutations and adds to the growing body of neurological disorders linked with altered protocadherins.

Patients and Methods

Patient Recruitment

Patients were identified from genetics and/or neurology clinics targeting patients with structural brain diseases or neurodevelopmental disorders in regions of the world displaying elevated rates of parental consanguinity. All patients/families enrolled in institutional review board–approved protocols and provided consent for study. The total cohort includes >6,000 individual families recruited between 2004 and 2017 presenting with features of intellectual disability, autism-related conditions, microcephaly, structural brain disorders, epilepsy, or neurodegeneration. The cohort was enriched for families with recessive pediatric brain disorders attributed to consanguinity (>80% of pedigrees) and multiple affected members (>60% of families). Routine medical records, history, physical and neurological examination, as well as evaluation of brain MR imaging (MRI) or CT were carried out as part of the standard clinic evaluation, and several patients underwent both modes of imaging. Determination of callosal abnormalities was based on visual observation by taking into consideration the age of each patient at the time of imaging. Pedigree analysis and blood sampling were pursued in all families, and subjects were selected for exome sequencing based upon a clinically defined neurodevelopmental genetic condition. Sequencing was performed on 1 or 2 affected patients or the father-mother-affected trio per family.

Exome Sequencing

Genomic DNA (gDNA) was extracted and subjected to exon capture, sequencing, variant calling, and computational filtering as previously described.[22] Briefly, gDNA was extracted (Qiagen [Hilden, Germany] or Oragene [DNA Genotek, Kanata, ON, Canada]) and subject to exon capture with the Agilent Sure Select Human All Exome 50Mb Kit (Agilent Technologies, Santa Clara, CA). Paired-end sequencing was with Illumina HiSeq2000 or HiSeq4000 instruments (Illumina, San Diego, CA),[23] resulting in 94% recovery at > 10 × coverage and 85% recovery at > 20 × coverage. The Genome Analysis Toolkit (GATK) was used for variant identification and then filtered for homozygous variants using Varvis software (Limbus Medical Technologies GmbH, Rostock, Germany), to deprioritize alleles with >0.1% frequency in control populations (in-house exome data set of 9,500 individuals, dbSNP, and ExAC Exome variant server), occurring outside of homozygous intervals in consanguineous families, or outside of linkage intervals. The remaining variants were ranked by the type of pathogenic variant (nonsense/splice/indel > missense), aa conservation across species, and damage prediction programs (PolyPhen and SIFT score).

Cell Transfection

Human full-length *PCDH12* was amplified from mammalian gene collection (MGC) fully sequenced complementary

DNA (cDNA) clone, cloned into either N-terminal FLAG-tagged mammalian expression vector, and mutagenized to incorporate patient mutations. 293T cells (ATTC, Manassa, VA) were transfected with the FLAG-tagged expression vectors using Lipofectamine 2000 (Thermo Fisher Scientific, Waltham, MA). Cell extracts were analyzed by western blotting with primary antibodies against FLAG (F7425; Sigma-Aldrich, St. Louis, MO) or α-tubulin (T6074; Sigma-Aldrich), detected by horseradish peroxidase–conjugated secondary antibodies and chemiluminescence (Thermo Fisher Scientific).

Fibroblast Culture, Induced Pluripotent Stem Cells, and Neural Progenitor Cell Generation

Primary fibroblast cell lines were established from unaffected and affected skin explants of dermal biopsies from family 1 (1592), according to standard methods. Induced pluripotent stem cells (iPSCs) were generated as previously described,[25] by episomal gene transfer of *cMYC, OCT4, KLF4*, and *SOX2.* Colonies with a healthy appearance (rounded smooth edges) were selected for further cultivation and evaluation. Neural progenitor cells (NPCs) were obtained as previously described,[26] with iPSCs cultured in serum-free floating embryoid body-like aggregates with 1mM of dorsomorphin (Tocris Bioscience, Bristol, United Kingdom), 2mM of A8301 (Tocris), and kept shaking at 95rpm for 7 days. Resultant embryoid bodies (EBs) were plated onto Matrigel-coated (BD Biosciences, San Jose, CA) dishes in neutral buffered formalin (NBF) medium (Dulbecco's modified Eagle's medium/F12, 0.5 × N2, 0.5 × B27, and 20ng/ml of basic fibroblast growth factor) to yield rosettes, which were dissociated with Accutase (Millipore, Burlington, MA) after 5 to 7 days, and resultant NPCs plated onto poly-ornithine/laminin–coated (POL; Sigma-Aldrich) dishes in NBF medium. Endothelial cells (ECs) were differentiated as previously described,[27] and iPSCs were cultured in serum-containing media in a nonadherent Petri dish for 13 days. Resultant EBs were dissociated to single cells and incubated with anti-CD31/fluorescein isothiocyanate (BD Pharmingen, San Diego, CA). Fluorescence-activated cell sorting (FACS) analysis to sort $CD31^+$ cells was performed on a FACSAria instrument (BD Biosciences), and resultant $CD31^+$ cells were plated onto 1% gelatin-coated dishes in endothelial growth medium-2 medium (Lonza, Basel, Switzerland). Experiments were performed with NPCs at passages four to six and ECs at passages three to five. Bright field images were taken in an EVOS microscope and processed with Photoshop CS5 (Adobe Systems, San Jose, CA).

Neurite Length Quantification

To determine neurite length, NPCs were plated on POL-coated dishes and transfected with phosphorylated enhanced green fluorescent protein (pEGFP) plasmid using Lipofectamine 2000 (Thermo Fisher Scientific). pEGFP-tagged NPCs were allowed to extend processes, then analyzed after 24 hours. Cells were fixed for 10 minutes with 4% paraformaldehyde, washed with phosphate-buffered saline, permeabilized with 0.15% Triton X-100, and blocked 1 hour in the same solution with 5% normal donkey serum. Slides were incubated with primary antibody (Nestin; 1:2,000; Millipore) overnight at 4°C and then incubated with fluorescently labeled secondary antibody (Jackson ImmunoResearch, West Grove, PA) for 2 hours at room temperature. Fluorescent signal was detected using an Olympus IX51 inverted microscope (Olympus, Tokyo, Japan) or Leica SP5 confocal microscope (Leica Microsystems GmbH, Wetzlar, Germany), then images were processed with Photoshop CS5 (Adobe). Length of the primary neurite per NPC was measured using FIJI/ImageJ (NIH, Bethesda, MD).

Results

Identification of Pathogenic Variants in PCDH12

In order to identify causes of DMJD, we first studied the originally reported families.[1] We performed whole-exome sequence (WES) analysis from 2 affected individuals in family 1 (originally described as family 1592), with prioritization of variants based upon established criteria[28] and <0.1% allele frequencies derived from an in-house exome database from ethnically matched individuals. We identified six variants of moderate-to-high impact (see Supplementary Table 1). Further filtering of variants for only "high impact" identified a single rare homozygous hg19: chr5:141334906delC variant in *PCDH12* (c.2511delG), a 1-base-pair (bp) deletion, leading to a frameshift (p.S838fs*; Fig 1A,B), which segregated according to a recessive mode of inheritance. Sanger sequencing of the coding region of *PCDH12* in the affected individuals of previously described family 2 (originally described as family 1846)[1] identified a hg19:chr5: 141334652delAG (c.2765delCT) 2-bp deletion leading to a frameshift (p.P922fs*). Of the three families originally described with DMJD,[1] all displayed evidence of the butterfly sign, families 1 and 2 showed lateral ventricles with typical size, and family 1825 showed massively dilated lateral ventricles. Consistent with that phenotypic difference, in family 1825 no *PCDH12* pathogenic variant was identified. The presumed role of *PCDH12* in cell-cell contact-dependent recognition made it an attractive candidate for DMJD, prompting further investigation.

We identified six additional families with pathogenic variants in *PCDH12.* WES analysis from our cohort of identified six additional *PCDH12* homozygous truncating

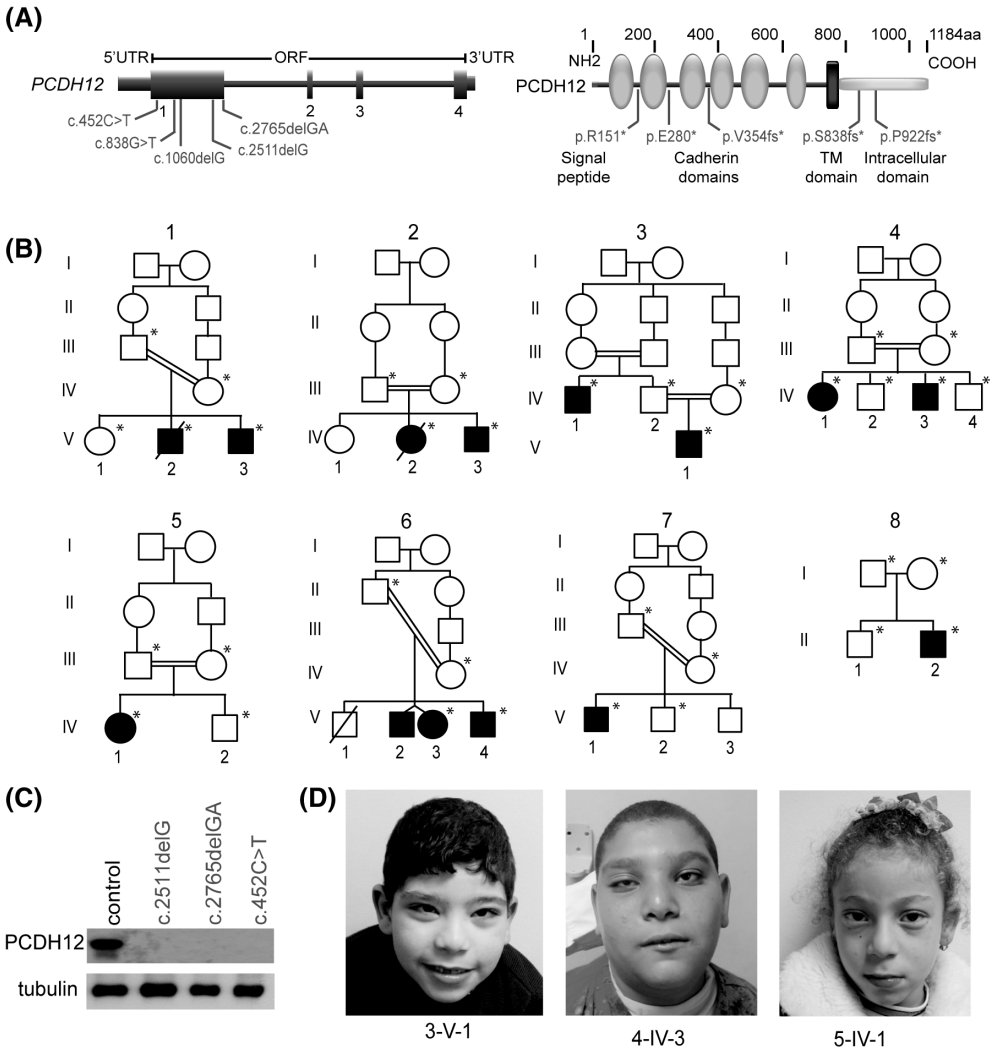

FIGURE 1: Biallelic pathogenic variants in *PCDH12* lead to microcephaly and spasticity. (A) Exons of PCDH12 with location of the patient pathogenic variants (top). Location of pathogenic variants relative to predicted protein (bottom). Cadherin domains (circle), transmembrane domain (TM). (B) Pedigrees of consanguineous families 1, 2, 3, 4, 5, 6, and 7 and nonconsanguineous family 8. (C) Impaired PCDH12 expression in 293T cells transfected with vectors encoding pathogenic variants c.2511delG, c.2765delCT, and c.452C>T. (D) Pictures of affected members from families 3, 4, and 5 showing the characteristic facial dysmorphism. Reproduced with permission of their parents. aa = amino acid; ORF = open reading frame; 3'UTR = 3' untranslated region.

pathogenic variants. Families 3 and 4 both displayed the homozygous 2-bp deletion (c.2765delCT) present in family 2, and family 5 presented with a nonsense pathogenic variant, hg19:chr5:141336579C>A (c.838G>T), leading to a premature stop codon (p.E280*; Fig 1A,B). No other prioritized variants segregated in any family (see Fig 1 and Supplementary Tables 2 and 3), leaving *PCDH12* as the top candidate for each family.

A second cohort of 2,000 subjects with neurodevelopmental disorders from the Yale Mendelian Sequencing Consortium was analyzed with WES and identified two additional consanguineous families with homozygous deleterious variants in *PCDH12.* Family 6 displayed an hg19: chr5: 1413336965G>A (c.452C>T) variant leading to a p.R151* premature stop codon, and family 7 displayed the same 2-bp deletion (c.2765delCT) found in families 2, 3, and 4. We identified an additional Moroccan Jewish nonconsanguineous family 8 presenting with a homozygous 1-bp deletion hg19:chr5:141336357delC (c.1060delG), p.Val354fs* (Fig 1A,B). Direct questioning showed no evidence of known shared ancestry for families sharing a common pathogenic variant. No correlation was detected between individual pathogenic variant and overall disease severity. No biases were detected in severity or age of onset based upon patient sex, and all pathogenic variants were fully penetrant without observed phenocopies within the family. Direct Sanger sequence confirmed segregation in all available family members according to strict recessive inheritance with full penetrance. To study the effect of patient pathogenic variants, we used point mutagenesis to

introduce c.2765delCT (most common variant), c.2511delG (example frameshift), and c.452C>T (example nonsense) in a plasmid containing full-length *PCDH12*. We found no protein expression after misexpressing mutated *PCDH12* constructs in 293T cells (Fig 1C). We conclude that the pathogenic variants tested result in lack of PCDH12 expression.

PCDH12 *Patients Show Microcephaly and Spasticity*

Clinical features of all 14 individuals from the original two families with *PCDH12* pathogenic variants and six new families are summarized in the Table and reported in detail in Supplementary Table 4. Recurrent fever of unknown etiology was observed in 64% of patients, with early onset and up to 2 months of age. Epilepsy was observed in 76% of patients with onset usually before 3 months of age and consisted of tonic, atonic, generalized tonic-clonic, and focal seizures, partially controlled with anticonvulsant medications. History of recurrent vasomotor instability was prominent in more than half of the patients (57%). The study included 10 males and 4 females, and ages ranged from 18 months to 6 years.

All patients presented with microcephaly and profound psychomotor delay. Head circumference was 1.5 to 8.7 standard deviations (SDs) below the mean, with almost 80% of patients (78%) in the range of 3 to 6 SDs below the mean. Head circumference at birth was available in 7 of 14 patients and ranged from 0.6 to 1.5 SDs below the mean, indicating predominantly postnatal progressive microcephaly. Bitemporal narrowing attributed to severe microcephaly was noted in half of patients. None was able to stand or walk independently, and none developed meaningful fine motor skills or language. Most patients displayed severe cognitive impairment, and 28% of patients presented with autistic features. Ataxia was present in 42% of patients. Pyramidal tract signs were evident in all; 64% of patients presented with hyperreflexia whereas the rest displayed truncal hypotonia (28%), and mild-to-severe appendicular spasticity was present in 28% of patients. Cranial nerve findings included strabismus (28% of patients), dysphagia (28% of patients), minimal-to-absent tracking of objects (21% of patients), and squinting (14% of patients). A combination of two or even three of these cranial nerve findings was observed in those more severely affected patients (1-V-2, 2-IV-2, and 3-IV-1). Facial dysmorphism was noted in most of patients (85%), which included low-set ears, broad prominent nasal bridge, long flat philtrum, broad chin, and thin upper lip (Fig 1D). Metabolic profile and echocardiography was normal in all patients evaluated.

Brain imaging was available in 12 of 14 subjects. Five patients underwent only MRI, whereas the other 7 had MRI plus CT head imaging. Brain imaging demonstrated a variety of brainstem malformations present in affected individuals in all families; including the DMJD pathognomonic butterfly-like contour of the midbrain on axial sections (Fig 2). Thin corpus callosum was frequently observed in patients and did not show more-severe thinning in older patients, arguing against progressive atrophy (Fig 3). Overall, cerebellum and pons were preserved and ventriculomegaly was present in 57% of patients. Our investigation did not reveal any overt vascular or coagulation phenotypes in patients (Supplementary Table 4), and MRI showed normal cerebral vascular flow voids, suggesting lack of detectable vascular defect. *PCDH12* pathogenic variants have been recently linked to brain calcifications[21]; therefore, we examined the available CT images. We found subtle brain calcifications in six of seven available CT studies (not shown), suggesting that calcifications can accompany DMJD attributed to *PCDH12* mutations.

PCDH12 *Is Involved in Neurite Outgrowth*

PCDH12 is expressed in several in human tissues, including the nervous system (Fig 4A), but expression was mainly documented in ECs; therefore, we used iPSCs to determine whether *PCDH12* is expressed in human neural cell linages. Fibroblast cultures from 2 affected and 1 carrier individual (heterozygous father) from family 1 were reprogrammed to iPSCs, verified upon expression of pluripotency markers and differentiation to three germ layers (not shown). *PCDH12* expression was undetectable in fibroblasts or iPSCs (not shown). Each iPSC line was differentiated into NPCs and ECs separately. All NPC clones expressed early neural stem cell markers PAX6 and nestin. Similarly, all endothelial cell clones expressed the endothelial markers, von Willebrand factor (vWF), calponin, and vinculin (Fig 4B). *PCDH12* showed expression in both neural and endothelial derivative cells. We obtained similar results from NPCs and ECs derived from three different iPSC clones subjected to two independent differentiation rounds for each individual.

PCDH12 was expressed in differentiated cells from control (wild-type) and unaffected (heterozygous) individuals, both in NPCs and ECs, but was undetectable in cells from affected individuals. This is in agreement with the analysis in cell culture (Fig 1C). Family 1 presented with c.2511delG, a pathogenic variant in the first exon leading to a predicted premature protein truncation, suggesting lack of *PCDH12* expression attributed to nonsense mediated decay. Moreover, all neural markers tested were exclusively found in NPCs, from both unaffected and affected individuals. Similarly, ECs from both unaffected and affected individuals expressed endothelial, but not

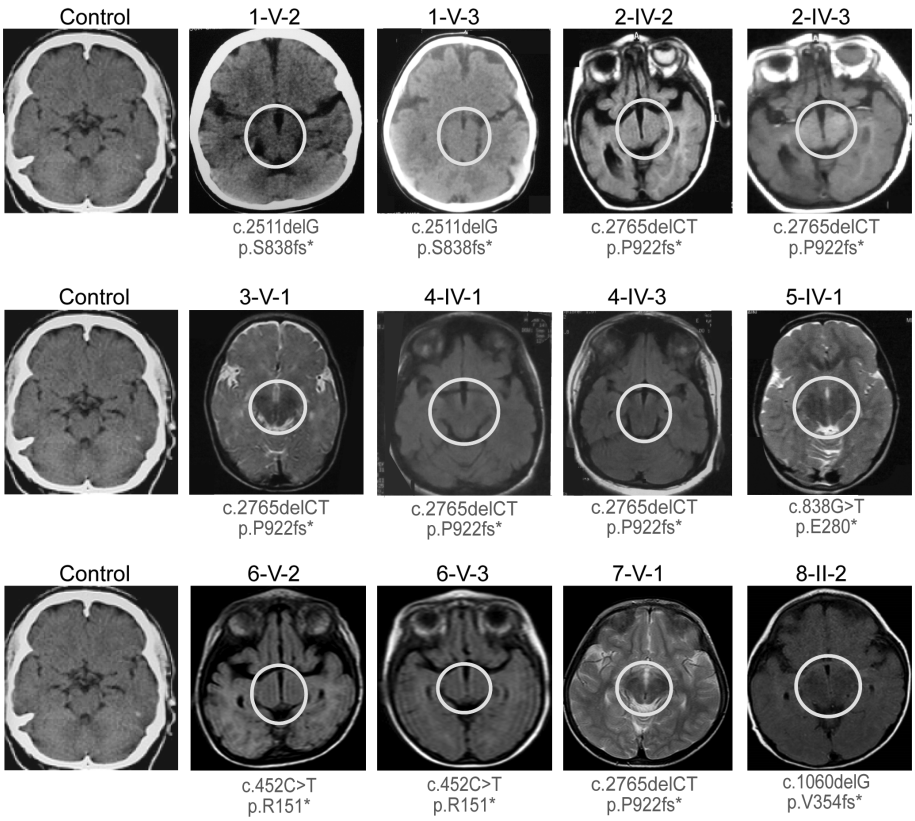

FIGURE 2: Biallelic pathogenic variants in *PCDH12* lead to brainstem malformations. Head computed tomography or brain magnetic resonance imaging of 12 affected individuals at the level of midbrain compared to control. All affected individuals showed brainstem malformations (circle). Butterfly sign was most obvious in the originally described families 1 and 2 (top row), consisting of an anterior midbrain cleft contiguous with the third ventricle. In other families in which *PCDH12* pathogenic variants were identified from sequencing, the butterfly sign was not obvious (eg, 5 and 8). *PCDH12* pathogenic variant in cDNA (c.) and protein (p.) corresponding to NM_016580 and NP_057664 Entrez IDs. cDNA = complementary DNA.

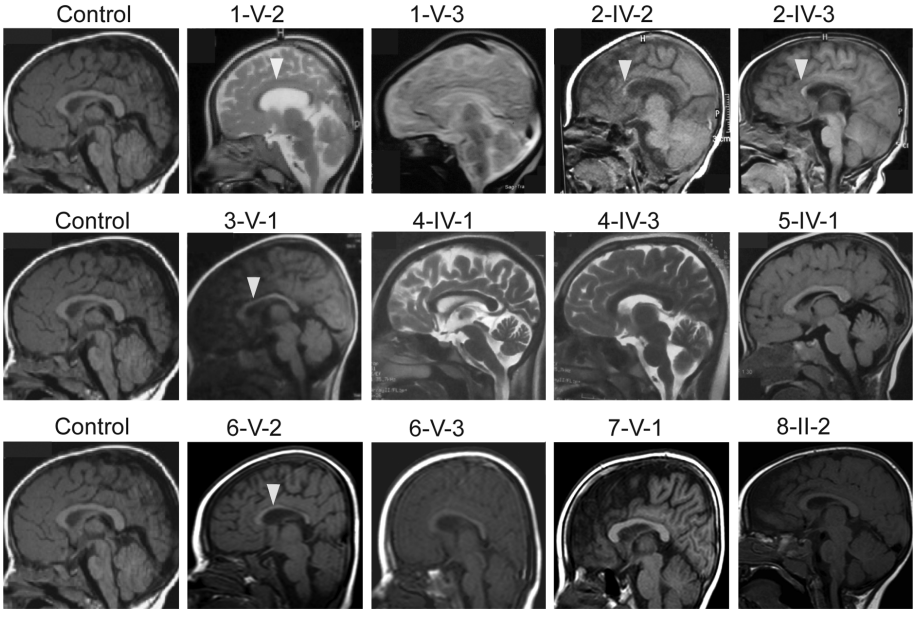

FIGURE 3: Biallelic pathogenic variants in *PCDH12* lead to defects in white matter tracts. Midline sagittal brain MRI showing thinned corpus callosum (arrowheads) in many of the affected individuals. MRI = magnetic resonance imaging.

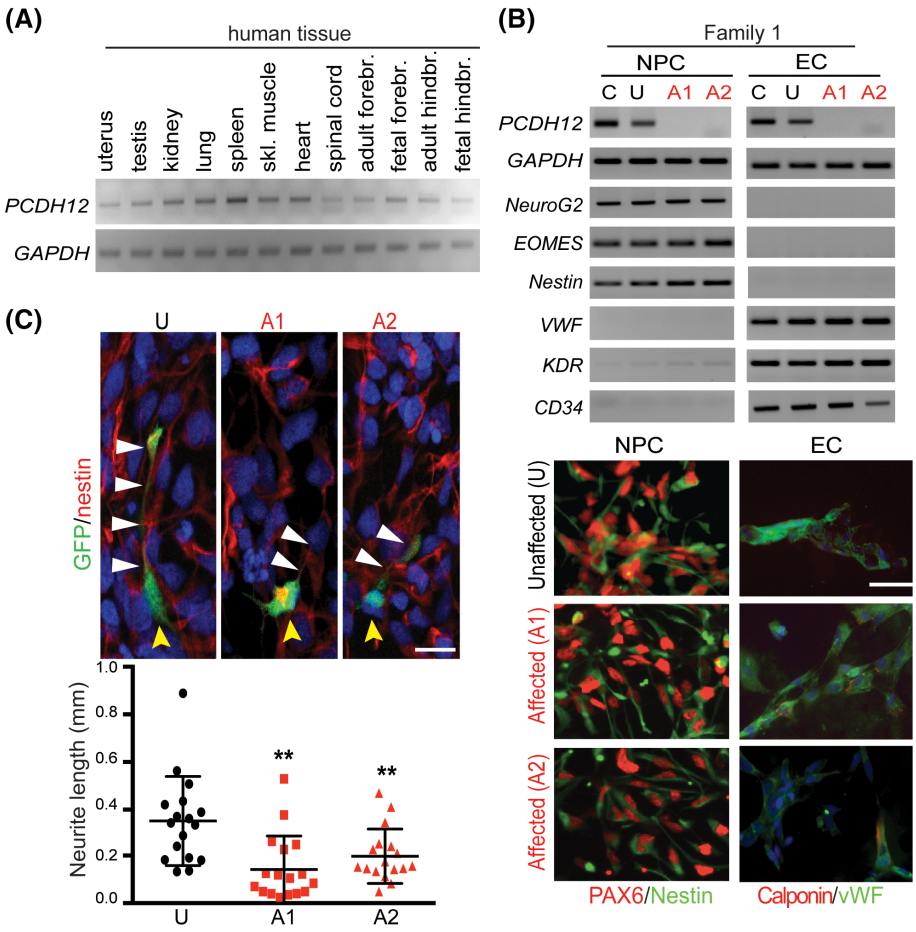

FIGURE 4: ***PCDH12*** **is expressed in several cell populations during human brain development. (A) RT-PCR of** ***PCDH12*** **showing ubiquitous expression across human tissues. (B) Neural precursor cells (NPCs) and endothelial cells (ECs) derived from unaffected (U) and affected (A1 and A2) members of family 1 are indistinguishable in differentiation. RT-PCR from NPCs and ECs showing** ***PCDH12*** **expression in control and unaffected, but not in affected cells. Differential expression of cell-specific markers is not dependent on the genotype. Isolated NPCs are PAX6 and nestin co-positive. Isolated ECs are calponin and vWF co-positive. No differences in immunostaining with neural and endothelial markers were observed. Scale bar, 40 μm. (C) Single GFP-labeled NPCs showing reduced neurite length in cells from affecteds lacking PCDH12 (A1 and A2) compared to unaffected (U), at high cell density. Neurite length averaged 0.38 in unaffected and 0.15 or 0.21 μm in affected (A1 and A2, respectively). Scale bar 10 μm. Red: nestin. Green: GFP-labeled neurite. Yellow arrowhead: cell body. White arrowheads: neurite. Mean ± SD. N ≥ 30 per genotype, ≥ 5 cells assessed in duplicates in three independent experiments. **$p < 0.05$, one-way ANOVA. ANOVA = analysis of variance; GFP = green fluorescent protein; SD = standard deviation; vWF = von Willebrand factor.**

neural, markers (Fig 4B). We conclude that *PCDH12* is expressed in both endothelial and neural lineages, and lack of *PCDH12* does not notably impact lineage differentiation.

Recently, it has been suggested that nonclustered protocadherins play roles in neurite outgrowth; therefore, we investigated the possible neural phenotypes caused by lack of PCDH12. We utilized dissociated NPCs in culture to investigate the role of PCDH12 in neurite outgrowth. We analyzed morphology of single NPCs plated at high density by sparse GFP labeling (ie, small percent of labeled cells). We found that mutant NPCs showed impaired neurite length (Fig 4C), suggesting that neurite outgrowth is dependent on PCDH12 expression.

Discussion

Protocadherins are implicated in the establishment and maintenance of neural circuits, and pathogenic variants in some protocadherin genes have been associated with neurodevelopmental and psychiatric disorders.[12–18,29] Although recent advances have aided our understanding of the molecular and cellular mechanisms related to protocadherin regulation of functional neuronal circuitry, key questions remain unanswered.

Here, we report on 14 cases in eight families with pathogenic variants in the nonclustered *PCDH12* in DMJD. Global developmental delay with severe cognitive impairment, hypotonia, dysmorphic facies, microcephaly, spasticity, and seizures were among the common features.

TABLE 1. Summarized Clinical Features of Patients With Pathogenic Variants in *PCDH12*

Clinical Finding	Patients, %
Microcephaly	100 (14 of 14)
Intellectual disability	100 (14 of 14)
Facial dysmorphism	92 (13 of 14)
Seizures	64 (9 of 14)
Recurrent unexplained fever	64 (9 of 14)
Vasomotor instability	57 (8 of 14)
Ataxia	42 (6 of 14)
Autistic features	
Pyramidal tract signs	28 (4 of 14)
Hyperreflexia	64 (9 of 14)
Spasticity	28 (4 of 14)
Hypotonia	28 (4 of 14)
Cranial nerve findings	
Strabismus	28 (4 of 14)
Dysphagia	28 (4 of 14)
Minimal to absent tracking	21 (3 of 14)
Squinting	14 (2 of 14)
Brain imaging findings	
DMJD	100 (14 of 14)
Corpus callosum hypoplasia	92 (13 of 14)
Brain calcification	85 (6 of 7)
Ventriculomegaly	57 (8 of 14)

DMDJ = diencephalic-mesencephalic junction dysplasia.

MRI studies obtained in affected individuals show a poorly defined diencephalic-mesencephalic junction with a characteristic malformation of the midbrain on axial sections. Additional imaging features include thinned corpus callosum and supratentorial calcifications.

Recently, a founder allele in *PCDH12* was identified in Palestinian families with congenital microcephaly and intracranial calcifications, mimicking a congenital infection.[20,21] The phenotype was reported similar to "intracranial calcifications with congenital microcephaly," which those investigators grouped with recessive conditions attributed to pathogenic variants in a tight junction component, occludin (*OCLN*; MIM#251290)[30] or junctional adhesion molecule 3 (*JAM3*; MIM#613730).[31] Here, we report that patients with *PCDH12* pathogenic variants not only present with calcifications and congenital microcephaly, but also abnormalities in white matter tracts. Consistent with these observations, we found *PCDH12* expression in both neural and endothelial cells. We performed brain MR tractography studies on a family with *OCLN*-related microcephaly and found no evidence of white matter defects, suggesting that the neural phenotype is not an obligate part of the brain calcification spectrum of conditions (not shown). Further studies are required to understand the precise role of *PCDH12* in brainstem development, or cross-talk between neurons and blood vessels during neural circuit formation.

In DMJD, MR tractography studies evidenced the CST originating within the cortex, but then failed to project through the ventral forebrain to reach the level of the brainstem, suggesting that the butterfly sign reflects a brainstem malformation with its origins in failed cortical projections. We identified additional patients with *PCDH12* pathogenic variants presenting with brainstem malformations, severe spasticity accompanied by paralysis, motor incoordination, and thinned corpus callosum, suggesting a generalized disruption of axonal tract formation. Development of mature axon tracts requires that axons navigate to find specific targets, but also that axons have a continuous outgrowth in order to reach the target. A defect in either event could result in abnormal tracts. Here, we found defective neurite growth attributed to loss of PCDH12 in NPCs derived from affected individuals. Therefore, we propose that individuals carrying *PCDH12* pathogenic variants display abnormalities in white matter tracts, possibly attributed to defects in neurite outgrowth. This is in agreement with extensive literature showing that nonclustered protocadherins play roles in neurite outgrowth. *PCDH7, PCDH10, PCDH17, PCDH18*, and *PCDH20* mediate axon growth and extension.[32–35] Moreover, *PCDH7, PCDH8*, and *PCDH10* are implicated in dendritic spine and synapse density[36] and *PCDH20* in conferring neuronal positioning.[29]

Understanding the roles of the family of nonclustered protocadherins in brain development will require further study and the use of different models, including iPSCs. Our data add PCDH12 to the members of nonclustered protocadherins family involved in the establishment and maintenance of neural circuits during nervous system development.

Acknowledgment

This work was supported by the NIH R01NS048453 and R01NS098004 to J.G.G., P30NS047101 for imaging support, K99NS089943 to A.G.-G., the Yale Center for Mendelian Disorders U54HG006504, RC2NS070477,

and the Gregory M. Kiez and Mehmet Kutman Foundation to M.G., Simons Foundation Grants 175303 and 275275, QNRF grant NPRP 6-1463-3-351 to J.G.G. and T.B.-O., and UM1 HG008900 to the Broad Institute of MIT and Harvard Center for Mendelian Genomics (Broad CMG).

We acknowledge the Yale Biomedical High-Performance Computing Center for data analysis and storage; the Yale Program on Neurogenetics and the Yale Center for Human Genetics and Genomics; the Center for Inherited Disease Research for genotyping; and the Simons Foundation Autism Research Initiative. Sequencing was provided, in part, by a gift from BGI and Illumina, Inc., to Rady Children's Hospital, San Diego for undiagnosed patients. Consortium for Autosomal Recessive Intellectual Disability (CARID) supported patient ascertainment.

Author Contributions

M.S.Z., M.G., and J.G.G. contributed to the conception and design of the study. A.G.-G., M.S.Z., A.O.-C., S.N.S., H.P., H.G., A.K.B., S.K., G.T.A., E.Z.E.-O., K.Y., K.B., H.G., N.P., N.S., D.W.-V., Y.P., R.O.R., B.B.-Z., A.G., N.A., A.O.-C., J.L.S., S.M.L., R.F., J.S., D.M., J.M.-V., D.B., B.C., S.G., and M.G. contributed to the acquisition and analysis of data. A.G.-G., V.S., and J.G.G. contributed to drafting the text and preparing figures, which was edited by all co-authors.

Potential Conflicts of Interest

Nothing to report.

References

1. Zaki MS, Saleem SN, Dobyns WB, et al. Diencephalic-mesencephalic junction dysplasia: a novel recessive brain malformation. Brain 2012; 135:2416–2427.
2. Abdel Razek AA, Castillo M. Magnetic resonance imaging of malformations of midbrain-hindbrain. J Comput Assist Tomogr 2016;40: 14–25.
3. Severino M, Righini A, Tortora D, et al. MR imaging diagnosis of diencephalic-mesencephalic junction dysplasia in fetuses with developmental ventriculomegaly. AJNR Am J Neuroradiol 2017;38: 1643–1646.
4. Madry J, Szlufik S, Koziorowski D, et al. The patient with mild diencephalic-mesencephalic junction dysplasia—case report and review of literature. Neurol Neurochir Pol 2017;17:30112–30113.
5. Wu Q, Maniatis T. A striking organization of a large family of human neural cadherin-like cell adhesion genes. Cell 1999;97:779–790.
6. Hulpiau P, van Roy F. Molecular evolution of the cadherin superfamily. Int J Biochem Cell Biol 2009;41:349–369.
7. Telo P, Breviario F, Huber P, et al. Identification of a novel cadherin (vascular endothelial cadherin-2) located at intercellular junctions in endothelial cells. J Biol Chem 1998;273:17565–17572.
8. Rampon C, Bouillot S, Climescu-Haulica A, et al. Protocadherin 12 deficiency alters morphogenesis and transcriptional profile of the placenta. Physiol Genomics 2008;34:193–204.
9. Rampon C, Prandini MH, Bouillot S, et al. Protocadherin 12 (VE-cadherin 2) is expressed in endothelial, trophoblast, and mesangial cells. Exp Cell Res 2005;302:48–60.
10. Hayashi S, Takeichi M. Emerging roles of protocadherins: from self-avoidance to enhancement of motility. J Cell Sci 2015;128: 1455–1464.
11. Kim SY, Yasuda S, Tanaka H, et al. Non-clustered protocadherin. Cell Adh Migr 2011;5:97–105.
12. Dibbens LM, Tarpey PS, Hynes K, et al. X-linked protocadherin 19 mutations cause female-limited epilepsy and cognitive impairment. Nat Genet 2008;40:776–781.
13. Marini C, Mei D, Parmeggiani L, et al. Protocadherin 19 mutations in girls with infantile-onset epilepsy. Neurology 2010;75:646–653.
14. Morrow EM, Yoo SY, Flavell SW, et al. Identifying autism loci and genes by tracing recent shared ancestry. Science 2008;321:218–223.
15. Tsai NP, Wilkerson JR, Guo W, et al. Multiple autism-linked genes mediate synapse elimination via proteasomal degradation of a synaptic scaffold PSD-95. Cell 2012;151:1581–1594.
16. Butler MG, Rafi SK, Hossain W, et al. Whole exome sequencing in females with autism implicates novel and candidate genes. Int J Mol Sci 2015;16:1312–1335.
17. Genetic determinants of common epilepsies: a meta-analysis of genome-wide association studies. Lancet Neurol 2014;13:893–903.
18. Chang H, Hoshina N, Zhang C, et al. The protocadherin 17 gene affects cognition, personality, amygdala structure and function, synapse development and risk of major mood disorders. Mol Psychiatry 2018;23:400–412.
19. Gregorio SP, Sallet PC, Do KA, et al. Polymorphisms in genes involved in neurodevelopment may be associated with altered brain morphology in schizophrenia: preliminary evidence. Psychiatry Res 2009;165:1–9.
20. Aran A, Rosenfeld N, Jaron R, et al. Loss of function of PCDH12 underlies recessive microcephaly mimicking intrauterine infection. Neurology 2016;86:2016–2024.
21. Nicolas G, Sanchez-Contreras M, Ramos EM, et al. Brain calcifications and PCDH12 variants. Neurol Genet 2017;3:e166.
22. Guemez-Gamboa A, Nguyen LN, Yang H, et al. Inactivating mutations in MFSD2A, required for omega-3 fatty acid transport in brain, cause a lethal microcephaly syndrome. Nat Genet 2015;47:809–813.
23. Gnirke A, Melnikov A, Maguire J, et al. Solution hybrid selection with ultra-long oligonucleotides for massively parallel targeted sequencing. Nat Biotechnol 2009;27:182–189.
24. Hoffmann K, Lindner TH. easyLINKAGE-Plus—automated linkage analyses using large-scale SNP data. Bioinformatics 2005;21: 3565–3567.
25. Okita K, Matsumura Y, Sato Y, et al. A more efficient method to generate integration-free human iPS cells. Nat Methods 2011;8: 409–412.
26. Chambers SM, Fasano CA, Papapetrou EP, et al. Highly efficient neural conversion of human ES and iPS cells by dual inhibition of SMAD signaling. Nat Biotechnol 2009;27:275–280.
27. Levenberg S, Ferreira LS, Chen-Konak L, et al. Isolation, differentiation and characterization of vascular cells derived from human embryonic stem cells. Nat Protoc 2010;5:1115–1126.
28. MacArthur DG, Manolio TA, Dimmock DP, et al. Guidelines for investigating causality of sequence variants in human disease. Nature 2014;508:469–476.
29. Depienne C, Bouteiller D, Keren B, et al. Sporadic infantile epileptic encephalopathy caused by mutations in PCDH19 resembles Dravet syndrome but mainly affects females. PLoS Genet 2009;5:e1000381.

30. O'Driscoll MC, Daly SB, Urquhart JE, et al. Recessive mutations in the gene encoding the tight junction protein occludin cause band-like calcification with simplified gyration and polymicrogyria. Am J Hum Genet 2010;87:354–364.

31. Mochida GH, Ganesh VS, Felie JM, et al. A homozygous mutation in the tight-junction protein JAM3 causes hemorrhagic destruction of the brain, subependymal calcification, and congenital cataracts. Am J Hum Genet 2010;87:882–889.

32. Uemura M, Nakao S, Suzuki ST, et al. OL-Protocadherin is essential for growth of striatal axons and thalamocortical projections. Nat Neurosci 2007;10:1151–1159.

33. Oishi K, Nakagawa N, Tachikawa K, et al. Identity of neocortical layer 4 neurons is specified through correct positioning into the cortex. Elife 2016;5. pii: e10907. doi: 10.7554/eLife.10907.

34. Hayashi S, Inoue Y, Kiyonari H, et al. Protocadherin-17 mediates collective axon extension by recruiting actin regulator complexes to interaxonal contacts. Dev Cell 2014;30:673–687.

35. Biswas S, Emond MR, Duy PQ, et al. Protocadherin-18b interacts with Nap1 to control motor axon growth and arborization in zebrafish. Mol Biol Cell 2014;25:633–642.

36. Keeler AB, Molumby MJ, Weiner JA. Protocadherins branch out: multiple roles in dendrite development. Cell Adh Migr 2015;9:214–226.